Progress In Electromagnetics Research M, Vol. 97, 57–68, 2020

Simplified Rectangular Planar Array with Circular Boundary for Side Lobe Suppression

Jafar R. Mohammed*

Abstract—The thinning methods were usually used to simplify the array complexity by turning off some of the radiating elements in large planar arrays which lead to unavoidable reduction in the directivity. In this paper, an alternative method is used to simplify the array complexity by partitioning a large array into two contiguous subarrays. The first subarray is in circular planar shape in which its elements are uniformly excited, while the second subarray in which its elements surround the circular subarray, and they have significant impacts on the array radiation features and are chosen to be adaptive. The desired radiation characteristics are then obtained by optimizing only the adaptive elements which are far less than the total number of the original array elements. Since the majority of the elements in the proposed array are uniformly excited, its directivity and taper efficiency are found very close to that of the benchmark solutions. Simulation results verify the effectiveness of the proposed array.

1. INTRODUCTION

Large planar antenna arrays have been used in many practical radar systems such as HAPDAR [1] which consists of 4300 elements, Cobra Dane [2] with 34768 elements, Pave Paws [2] which consists of 2677 elements, Sea Based X-Band radar [3] with more than 45000 transmit/receive modules, and the European Incoherent Scatter Scientific Association (EISCAT) radar based antenna arrays composed of more than 10000 elements [4]. In addition, the fifth generation (5G) wireless communication systems are also recommended for massive MIMO systems which consist of large antenna arrays to fulfil the increasing demands for higher speed and data traffic. Generally, the cost and complexity of the feeding network of such systems are very high. There are many approaches to simplify the feeding complexity. Among these approaches are those of thinning arrays where the redundant elements could be removed (turning off) from the original large arrays [5–7]. The feeding complexity can also be simplified by controlling only the phase excitations [8] or controlling the amplitude excitations of the array elements [9]. Recently, array pattern synthesis has been performed by using various global optimization methods such as genetic algorithm [10], particle swarm optimization [11–13], and differential search algorithm [14] in which the excitation amplitudes, phases, and/or element positions are taken as the optimization parameters. Very recently, the sparseness techniques via compressed sensing were also used to effectively minimize the number of array elements and simplify the feeding complexity [15, 16].

More effective solutions can be obtained by choosing only part of the array elements to be optimizable instead of all of them [17, 18]. The excitations of the elements of the non-optimized subarray are kept unchanged from their original excitations. In [19–23], various analytical and numerical techniques for array pattern optimization have been suggested, and they are basically based on partially adaptive arrays to simplify the array complexity. In [24], a small number of edge elements on both sides of a linear array are optimized to meet the required radiation patterns with controlled nulls. The

Received 29 June 2020, Accepted 4 September 2020, Scheduled 29 September 2020

* Corresponding author: Jafar Ramadhan Mohammed (jafar.mohammed@uoninevah.edu.iq).
The authors are with College of Electronic Engineering, Ninevah University, Mosul 41002, Iraq.

excitations of the inner elements of the linear array remained unchanged from their original excitations. Thus, the complexity of the array feeding network has been greatly reduced.

In this paper, the technique that was presented in [24] is extended to rectangular grid antennas with circular boundary elements to simplify the array complexity by partitioning a large array into two contiguous subarrays. Since the majority of the elements in the proposed array are uniformly excited, its directivity and taper efficiency are found very close to that of the benchmark solutions. The technique involves, first, forming a sub-rectangular planar array with circular boundary from an original rectangular array. The elements located inside the constructed circular aperture are chosen to be non-adaptive, while the surrounding (or outside the circle) elements which are characterized to have prominent features on the array radiation pattern are chosen to be adaptive. In addition, the diameter (i.e., in terms of number of the array elements within the circle) of the constructed circular aperture is also chosen to be adaptive such that a good compromise (trade-off) between the array complexity and optimized radiation pattern is obtained. The criteria used to divide the large array into two subarrays depend on the required constraint mask such as peak sidelobe level. In general, an adaptive subarray with a reasonable set of outer elements around the circle can offer a reasonable number of degrees of freedom to perform the sidelobe reduction in the overall array pattern. The number of degrees of freedom, however, should be significantly less than the total number of original array elements.

Then, by optimizing the amplitude excitations of the surrounding elements, one could cancel or reduce all the sidelobes on both azimuth and evaluation planes with capability to generate the required nulls at undesired directions. In order to get optimum suppression of sidelobes while maintaining the main beam undistorted, the genetic algorithm is used to find the optimal values of the amplitude excitations of the surrounded elements.

2. THE PROPOSED PLANAR ARRAY

The structure of the proposed planar array is shown in Fig. 1. It consists of a number of uniformly excited elements inside a circle with radius R and another number of adaptive elements surrounding the circular aperture. The details of each part are shown in the next subsections.

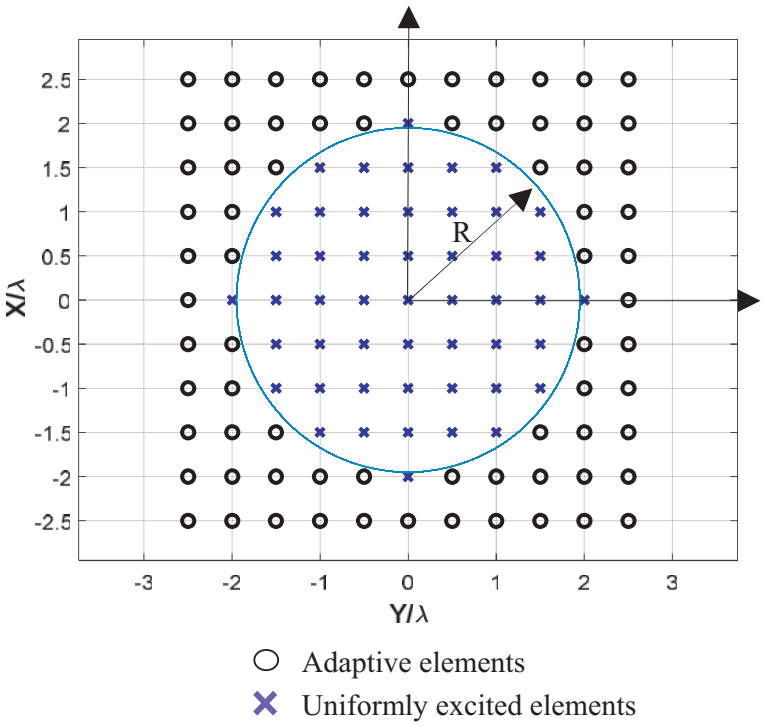

Figure 1. Structure of the proposed array.

2.1. Rectangular Array with Circular Boundary

Consider an initial $N \times N$ square grid as shown in Fig. 1. The array factor of such a planar array at the far field observation point can be given by [22]

$$\mathrm{AF}\,(\theta,\varphi) = \sum_{n=1}^{N}\sum_{n=1}^{N} a_{nn} e^{j\frac{2\pi d_x}{\lambda}[(n-1)(\sin\theta\,\cos\varphi)]} e^{j\frac{2\pi d_y}{\lambda}[(n-1)(\sin\theta\,\sin\varphi)]} \tag{1}$$

where θ and φ are the elevation and azimuth angles, respectively; $d = d_x{=}d_y{=}\lambda/2$ are the uniform inter-element spacings in x and y directions; and a_{nn} is the amplitude weighting of the initial planar array which could be uniform or nonuniform tapering distributions. The elements of the initial rectangular planar array is first partitioned into two unequally groups by drawing a circle centred at the origin with a certain radius, R, as shown in Fig. 1.

The elements located inside the circle are all kept unchanged from their original excitations, while the elements located outside the circle and on the sides of the rectangular array are optimized by means of genetic algorithm such that the main beam direction and the shape of the proposed array pattern are maintained as close as possible to that of the original rectangular planar array with some constraints on the sidelobe level and null controls during the optimization process of the outer elements.

To proceed with the proposed technique, first we need to find a proper value of radius, R, and the distance from the origin to any element, say $(n,\ n)$, in the initial planar array. R in terms of array elements, N, can be easily found as:

$$R = \frac{N-1}{2} + \delta \tag{2}$$

where δ is set to $\delta \leq \frac{d}{4}$. Then, the amplitude excitations, a_{nn}, in Equation (1) can be modified to

$$a_{nn} = \begin{cases} 1 & \text{if distance} < R \\ b_{nn} & \text{elsewhere} \end{cases} \tag{3}$$

Then Eq. (1) can be rewritten as shown below

$$\mathrm{AF}\,(\theta,\varphi) = \underbrace{\sum_{n=1}^{N_C} e^{j\frac{2\pi d}{\lambda}[(n-1)(u+v)]}}_{\text{elements inside the circle}} + \underbrace{\sum_{n=N_C+1}^{N} b_n e^{j\frac{2\pi d}{\lambda}[(n-1)(u+v)]}}_{\text{elements ouside the circle}} \tag{4}$$

Note that the array factor given in Eq. (4) is expressed as a one-dimensional sum instead of two-dimensional sum for the purpose of efficient programming. Here, N_C is the total number of elements inside the circle.

As mentioned earlier, the element excitations inside the circle are non-adaptive (or constant) while those outside the circle are adaptive. Thus, the complexity, in terms of the required number of adaptive elements compared to those of the fully adaptive planar arrays may be computed by the ratio of the number of the elements outside the circle (whose amplitude excitations are adaptive) to the total number of elements. Generally, it is found that a better reduction in the complexity can be obtained for larger circular apertures. That is large values of radius, R, for instance, an array with size of 9×9 elements and for $R = 4.025$ elements. The number of adaptive elements is 53 out of 81 total elements, and thus, the complexity is 65.43%.

2.2. The Cost Function

The cost function that is used to optimize the array power pattern according to the given upper and lower bounds of the constraint masks is described by

$$\text{cost} = \sum |\mathrm{AF}\,(\theta_s,\varphi_s) - \text{Mask Limit}|^2 \tag{5}$$

where $\mathrm{AF}(\theta_s, \varphi_s)$ represents the magnitude of the sidelobe pattern of the array factor of Eq. (4). The cost minimizes the sidelobe magnitudes that excess the constraint mask. Clearly, better solution can be obtained with lower cost. Each pattern point of $\mathrm{AF}(\theta_s, \varphi_s)$ that lies outside the particular mask limits

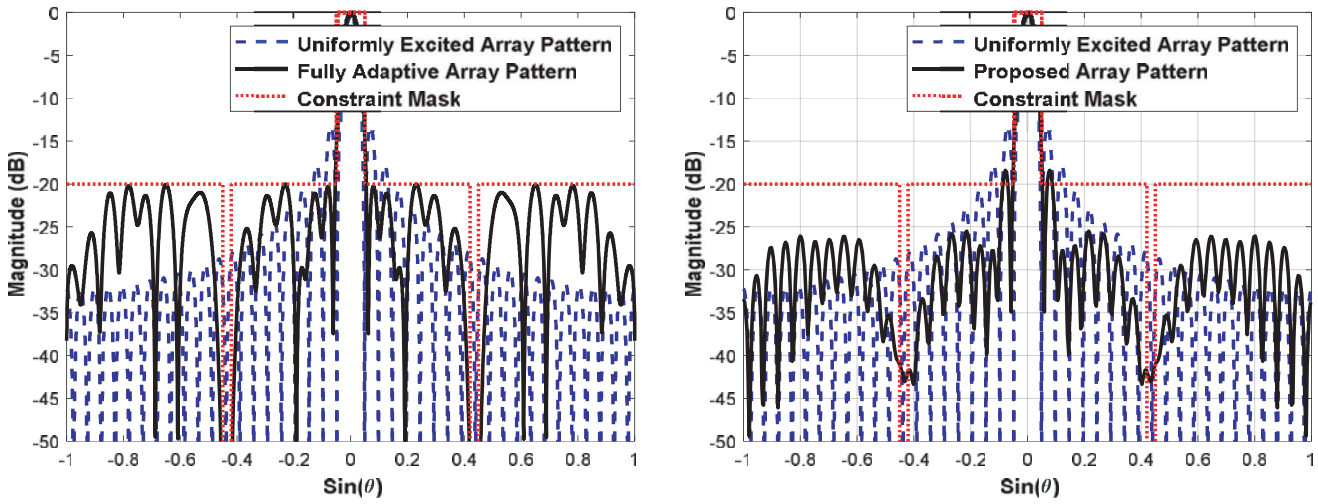

Figure 2. Cost functions for both fully adaptive array and the proposed array.

contributes a value to the cost function equal to the power difference between the desired constraint mask and the resultant array pattern. In other words, the constraint mask specifies the desired radiation characteristics. Then, the cost function can be defined as the square of the difference between the resulting array pattern and the desired one.

Figure 2 shows the results of applying the cost function shown in Eq. (5) to an array with fully adaptive elements and the proposed array with outer elements being adaptive only. The array size was $N \times N = 41 \times 41$ elements, and the number of the adaptive elements in the proposed array was 884. For both patterns, the required sidelobe mask was -20 dB, and a single null centred at $u = 0.435$ with width equal to 0.03 is considered. It can be seen that the proposed array pattern meets the desired constraint mask as the fully adaptive arrays are with much simplified array complexity.

3. SIMULATION RESULTS

In this section, extensive simulation results are demonstrated to illustrate the effectiveness of the proposed rectangular array with circular boundary and partially adaptive elements. To evaluate the performances of the standard fully adaptive rectangular array and the proposed array, the taper efficiency and average sidelobe level are computed as:

$$\eta = \frac{\left|\sum_{n=1}^{N}\sum_{m=1}^{M} a_{mn}\right|^2}{NM\sum_{n=1}^{N}\sum_{m=1}^{M}|a_{mn}|^2} \tag{6}$$

where η is the obtained taper efficiency which represents a measure of how efficiently the physical area of the considered planar array was utilized.

The average side lobe level is defined as the radiation pattern outside the main beam when it is summed and averaged with respect to the number of positions outside the main beam. This measure gives more insightful information about the reduction of the whole side lobe structure than the only peak side lobe level.

The main parameters of the used genetic optimization algorithm are set to be: selection was roulette; population size was set to 20; mutation rate was 0.15; crossover was single point; mating pool was set to 4. The amplitude-only weighting is used to find the optimized values of the adaptive elements. The lower and upper bounds of the adaptive elements were set to 0 and 1 while the phases are set to zero. Different numbers of array elements ranging from medium to large array sizes are demonstrated.

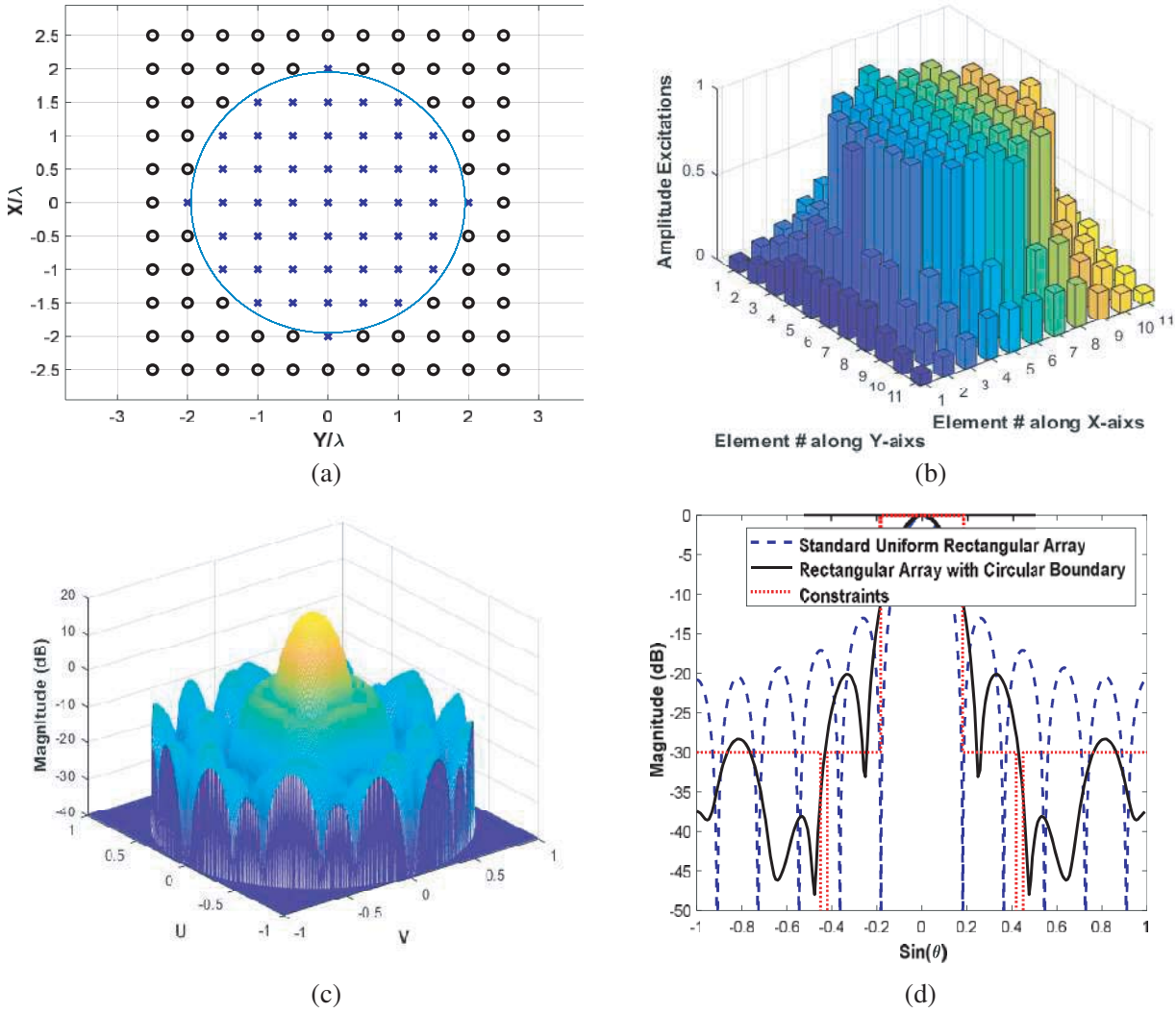

Figure 3. Results of the proposed array with uniform distribution for 11×11 elements and $R = 4.02$.

Example 1: Uniformly excited array with size 11×11

In this example, an initial rectangular array with size 11×11 elements is considered. The radius of the circle is chosen to be $R = 4.025$, and consequently, the number of non-adaptive elements located inside the circle is 49, while the number of surrounding adaptive elements is 72. Figs. 3(a) and (b) show the elements layout and the excitations of both adaptive and non-adaptive elements. The three and two-dimension radiation patterns of the proposed planar array and the standard uniformly excited planar array are shown in Figs. 3(c) and (d). In this case, the constraint mask consists of placing a null centred at $(u, v) = (0.435, 0.435)$, and the peak side lobe level should not exceed -30 dB in both u and v planes, main beam pointing at $(u, v) = (0, 0)$, and first null-to-null beam width should not exceed $(u, v) = (0.1667, 0.1667)$. It can be seen that the proposed rectangular grid with a circular boundary of radius $R = 4.025$ is capable to fulfil most of the desired constraints. On the other hand, the directivity of the proposed array is found to be 20.5537 dB, while that of the uniformly excited array was 21.9031 dB. Also, the taper efficiency of the proposed array was 2.1939. Moreover, the computational complexity of the proposed array is found to be 59.5% which is lower than that of the fully adaptive rectangular array by 40.5%.

Example 2: Uniformly excited array with size 21×21

In this example, the size of the initial rectangular array is chosen to be 21×21 elements, and the

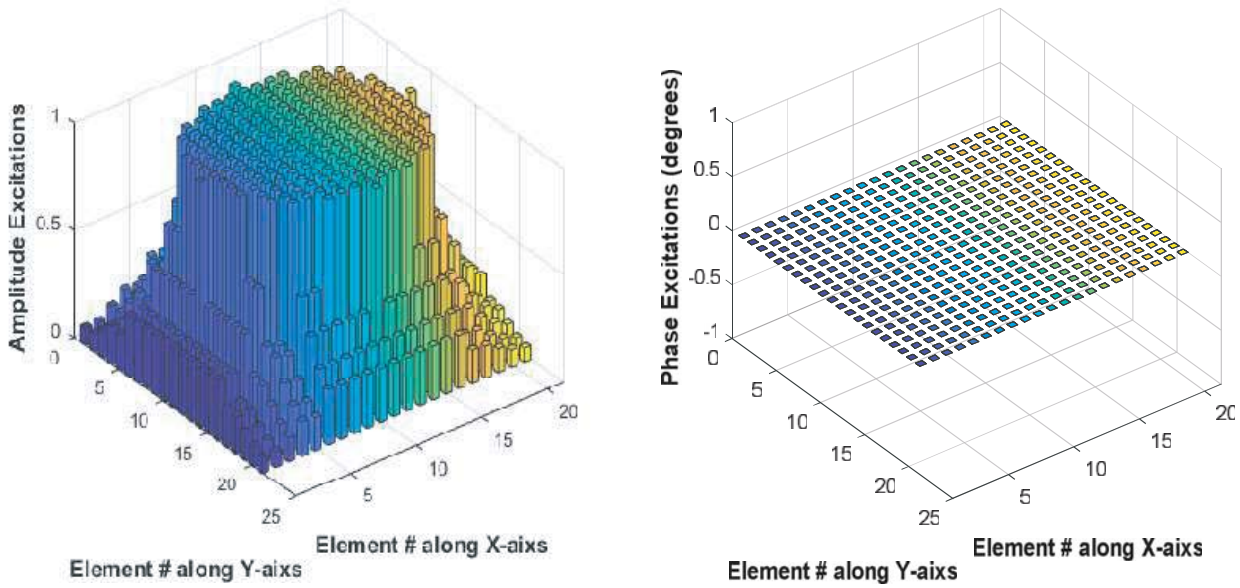

Figure 4. Amplitude and phase excitations of the proposed array for 21×21 elements and $R = 8.025$.

radius of the circle is chosen to be $R = 8.025$. Consequently, the numbers of non-adaptive and adaptive elements are 197 and 244, respectively. Fig. 4 shows the amplitude and phase excitations of the adaptive and non-adaptive elements, while Fig. 5(a) shows the element layouts, and Figs. 5(b) and (c) show the two and three-dimension radiation patterns of the proposed planar array with its corresponding contour (see Fig. 5(d)). The constraint mask was as in the previous example. For comparison purpose, the results of the fully adaptive planar array with size 21×21 are shown in Fig. 6. It can be seen that almost the same performance can be obtained with the proposed array at much lower computational complexity in the number of adaptive elements 55.33%. Moreover, the performance indicators of the proposed array under various radius values are listed in Table 1. For this array and for $R = 8.025$, the directivity and taper efficiency of the proposed array were 26.3223 dB and 1.9778, respectively, while for fully adaptive arrays, these values were 25.9502 dB and 4.9851. From these results, it is clear that the performance of the proposed array with partially adaptive elements is much better than that of the fully adaptive array elements.

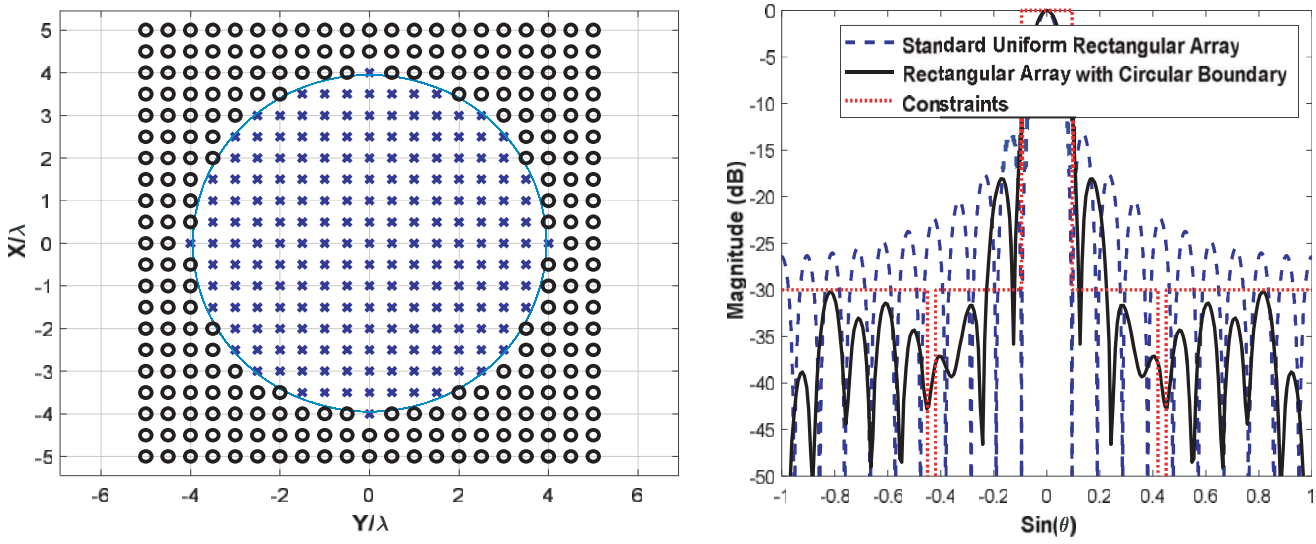

(a) (b)

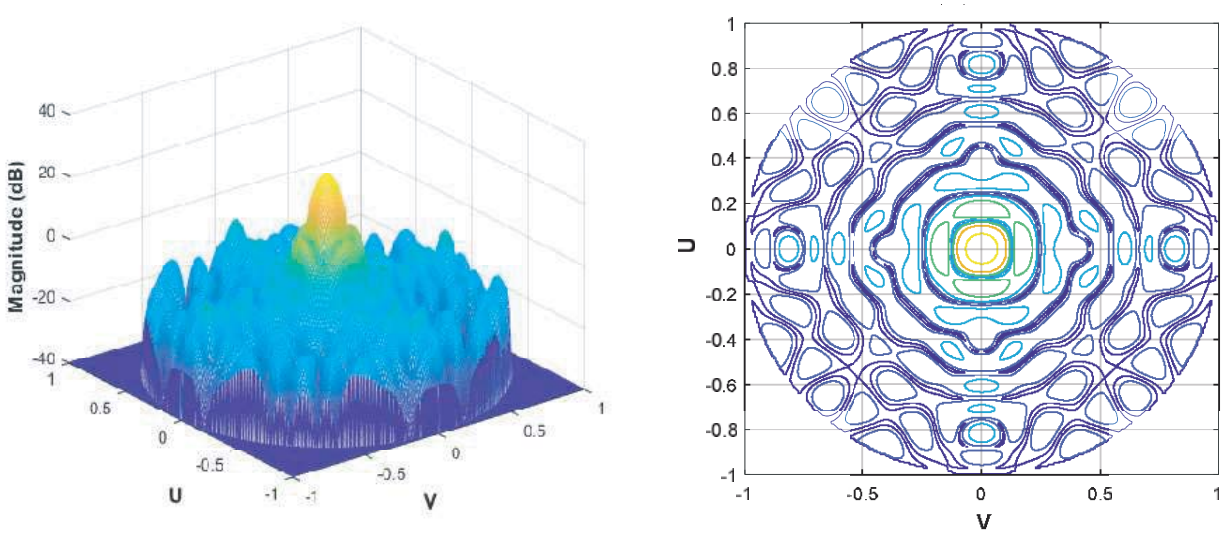

(c) (d)

Figure 5. Results of the proposed array for 21×21 elements and $R = 8.025$.

Table 1. Performance indicators versus radius, R, for 21×21 array elements.

Radius, R	Directivity (dB)	Taper efficiency	Peak side lobe level (dB)	Average side lobe level (dB)	Complexity %
	Standard uniformly excited rectangular array				
	27.5008	1	−13.23	−20.3320	0
	Proposed uniformly excited rectangular array with circular boundary				
10.025	27.4232	1.1254	−13.5	−21.1595	28.12
9.025	27.0727	1.4554	−17.0	−22.4610	42.63
8.025	26.6832	1.8406	−18.0	−23.1834	55.33
7.025	26.2762	2.0965	−20.0	−23.4178	66.21
6.025	26.6602	2.3683	−22.0	−25.1944	74.38
	Standard non-uniform (Dolph) excited array				
	27.0504	2.6746	−20	−19.3583	100
	Proposed non-uniform (Dolph) excited array with circular boundary				
10.025	26.8666	1.3178	−14.7	−21.3985	28.12
9.025	26.6969	1.5841	−17.5	−22.9208	42.63
8.025	26.1856	2.0263	−20.5	−24.7000	55.33
7.025	25.2923	2.6198	−20.8	−24.2784	66.21
6.025	25.3280	3.1061	−25.0	−26.8202	74.38

Example 3: Uniformly excited array with size 41×41

In this example, the size of the initial rectangular array is further increased to 41×41. Fig. 7 shows the results of the tested arrays. Again, the proposed array is capable to meet all the desired constraints. For this example, the directivity of the proposed array is found to be 32.3533 dB, while

that of the uniformly excited array was 33.3067 dB. Also, the taper efficiency of the proposed array was 1.8314 which is close enough to that of the uniformly excited array.

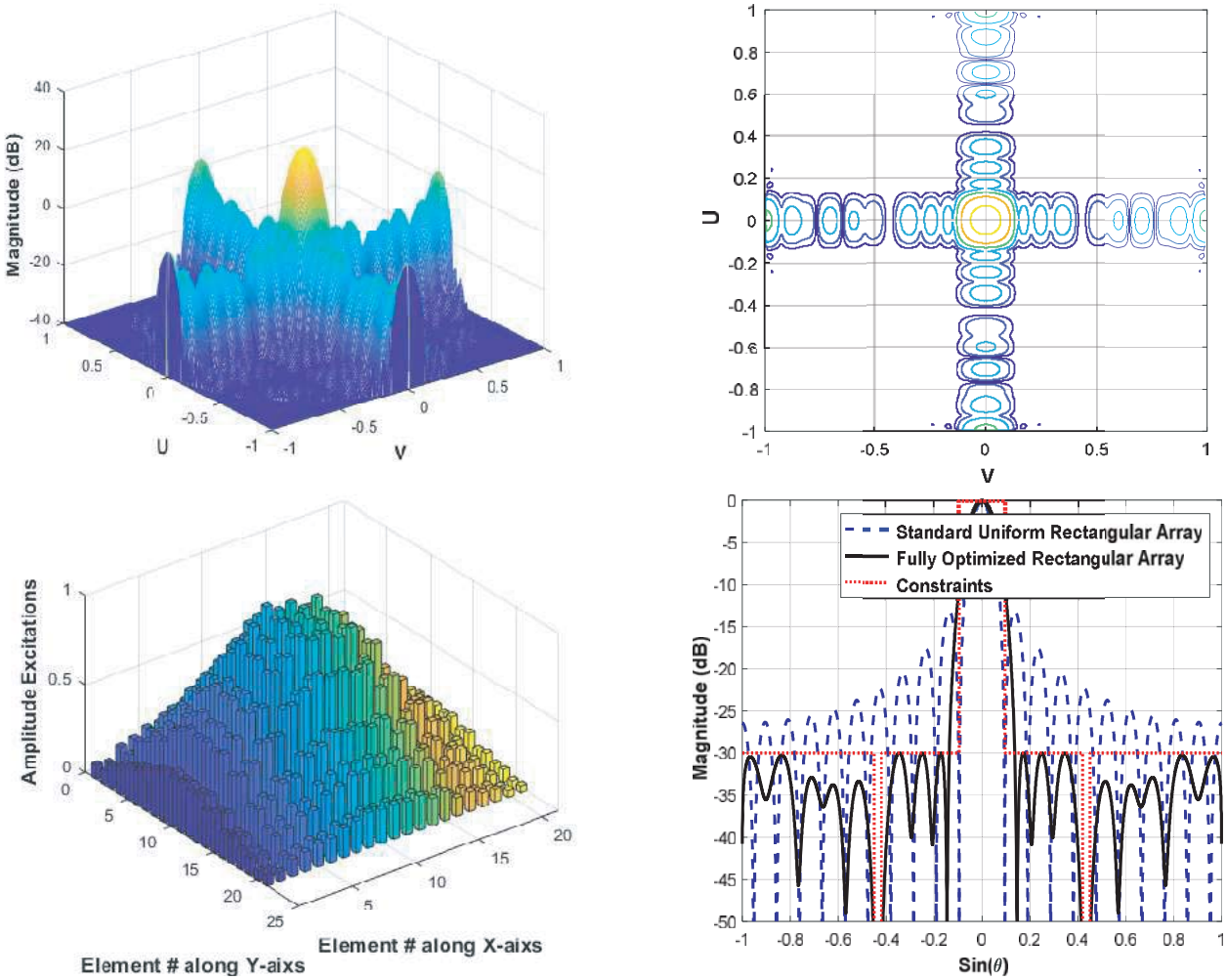

Figure 6. Results of the fully adaptive array for 21×21 elements.

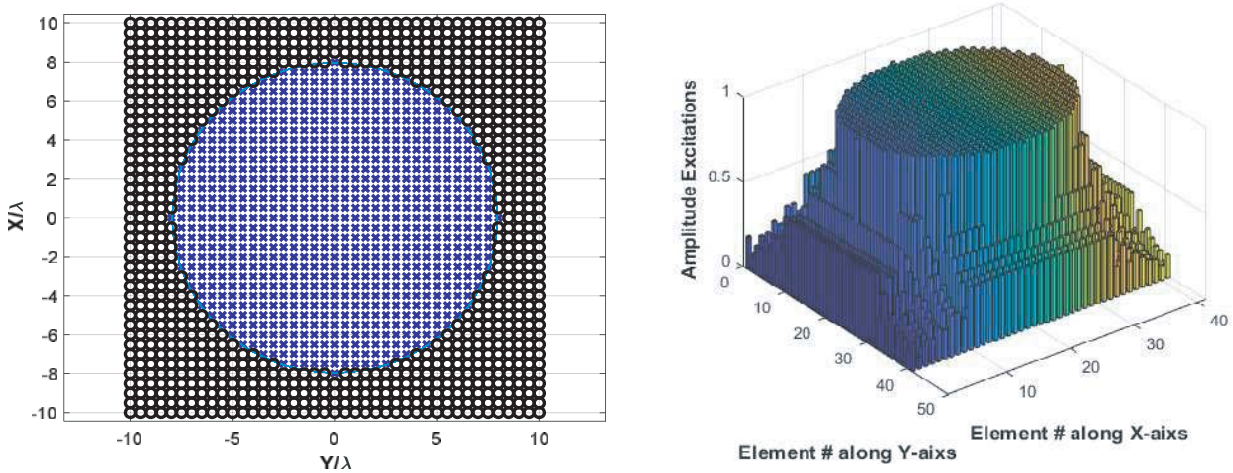

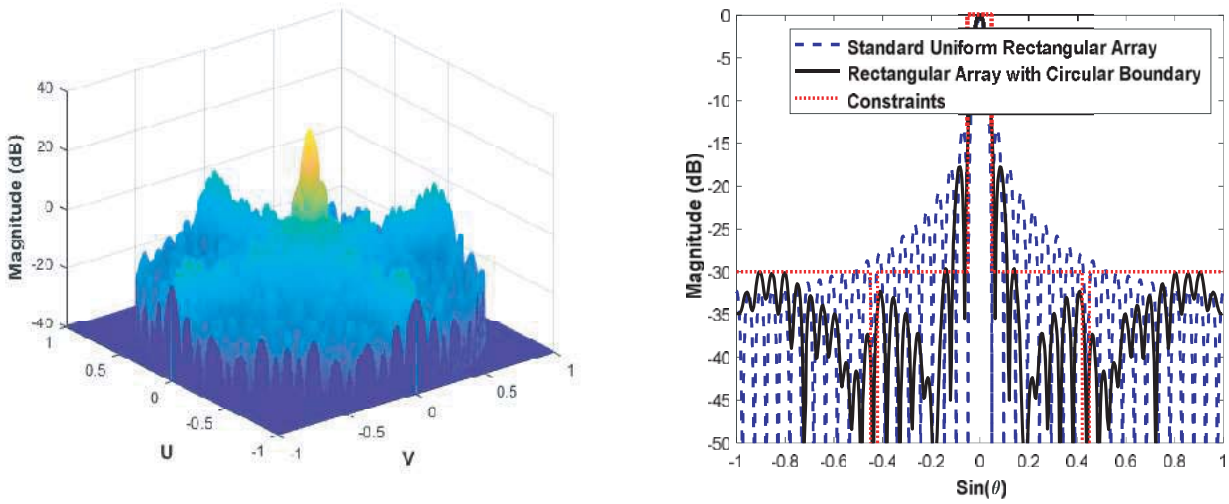

Figure 7. Results of the proposed array for 41×41 elements and $R = 8.025$.

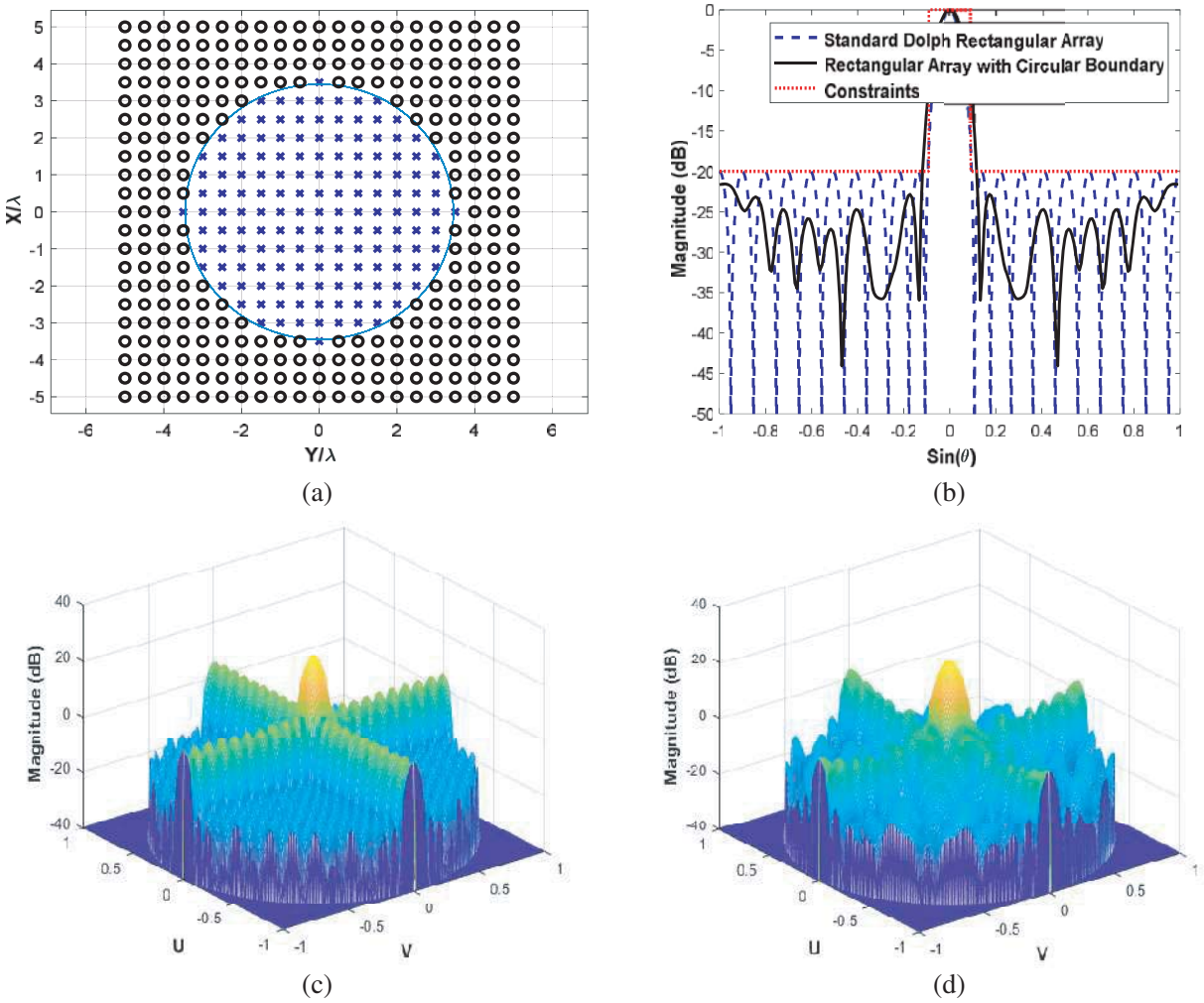

Figure 8. Results of the proposed array with Dolph distribution and for 21×21 elements and $R = 7.025$. (a) Array layout, (b) 2D array patterns, (c) original Dolph pattern, (d) proposed array pattern.

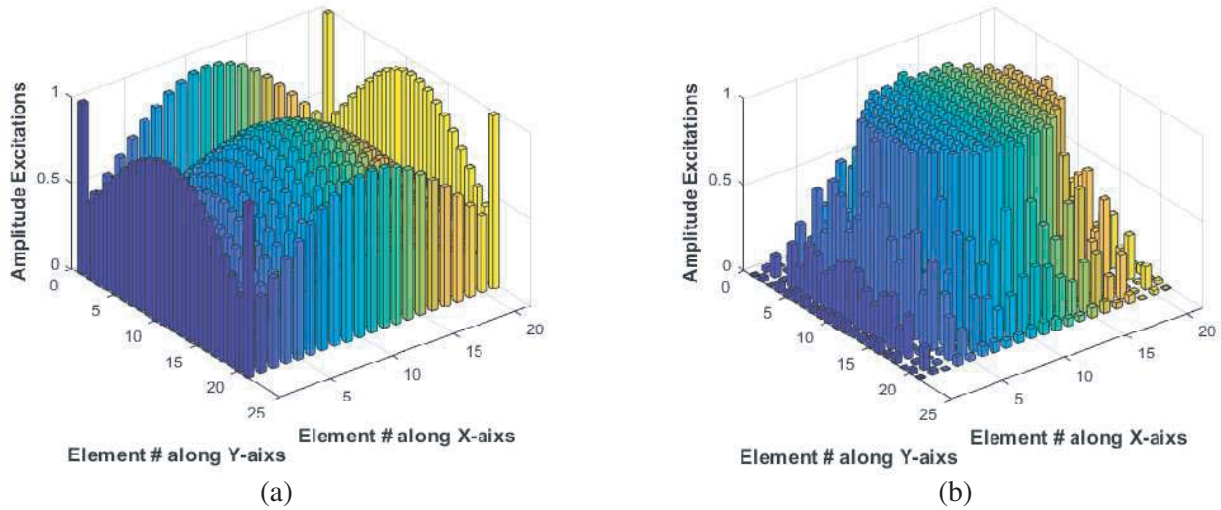

Figure 9. Amplitude distributions for (a) the original Dolph array and (b) the proposed array.

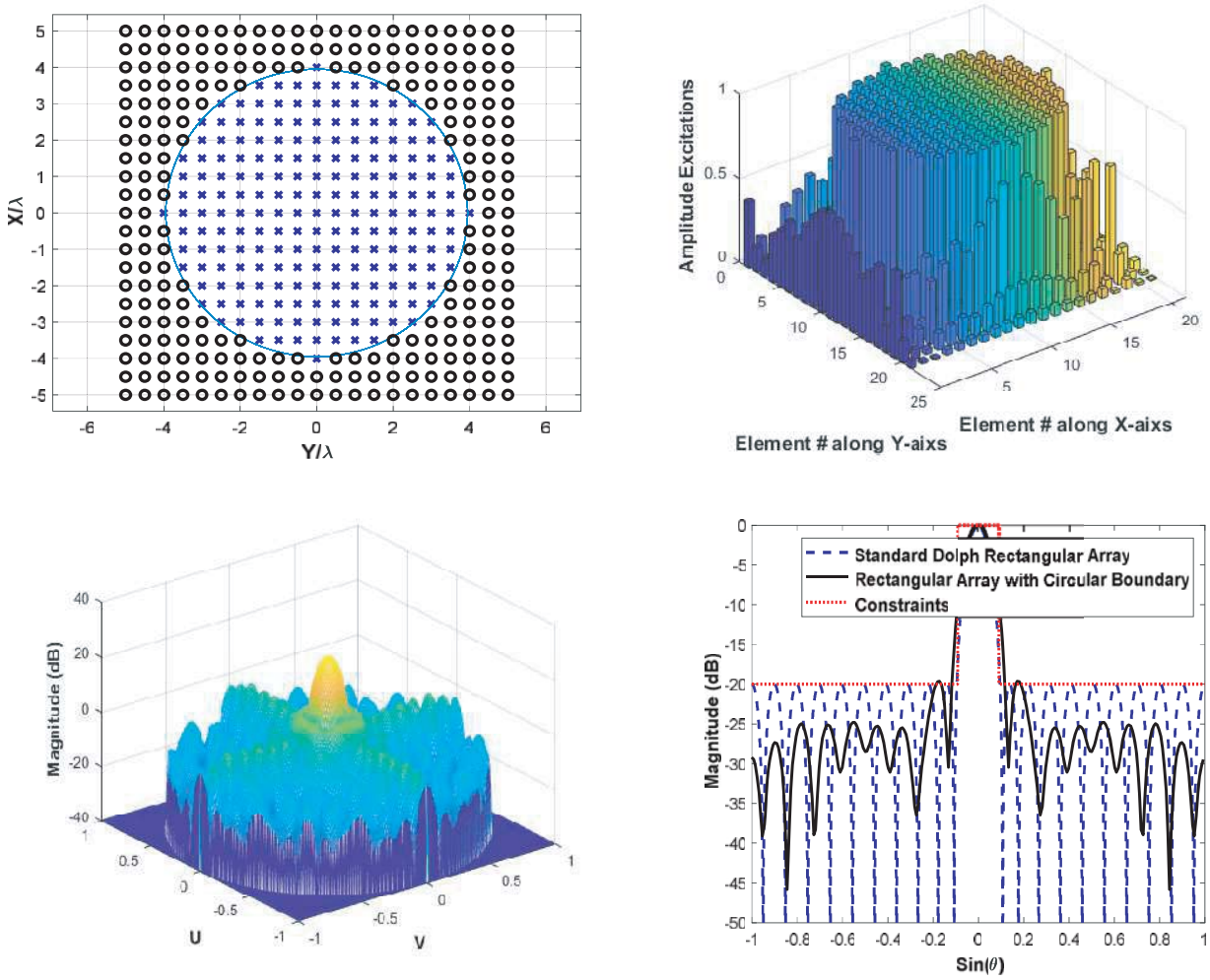

Figure 10. Results of the proposed array with Dolph distribution and for 21×21 elements and R=8.025.

Example 4: Dolph excited array with size 21×21

In this example, the proposed array is applied to the non-uniformly excited planar arrays such as Dolph array. Fig. 8 shows the elements layout for $R = 7.025$ and the corresponding radiation patterns of the standard Dolph array (21×21 elements, SLL $= -20$ dB) in which the excitations of the surrounding adaptive elements are only optimized to get radiation characteristics as close as to that of the standard fully adaptive Dolph array with simplified array feeding network. The amplitude excitations of the circular array elements were also set to ones. Fig. 9 shows the amplitude excitations of the standard Dolph excited array and the proposed rectangular array with circular boundary. Fig. 10 repeats the results of the proposed array for another value of $R = 8.025$. These results fully confirm the effectiveness of the proposed method in both uniform and nonuniform amplitude excitation arrays.

Finally, the effect of the number of adaptive elements (or the variations of the circle radius, R) on the directivity, taper efficiency, peak side lobe level, average side lobes, and the complexity of the feeding network in terms of the number of used adaptive elements are investigated for both uniformly and non-uniformly excited arrays. The results are shown in Table 1. It can be seen that the directivity and taper efficiency values of the proposed array are slightly degraded when the radius of the circle is reduced (i.e., increasing the number of adaptive elements). On the other hand, the peak side lobe level and average side lobe level are both significantly reduced with increased number of adaptive elements; of course, this comes at the cost of higher complexity. From these results, it can be concluded that simplifying the element excitations of a circular array on a square grid is a good option for practical radar systems.

4. CONCLUSION

It has been shown that the proposed technique represents a good solution for simplifying the large arrays. For the fully optimized rectangular array with size 21×21 adaptive elements, its performance indicators were found to be: taper efficiency = 4.7702, directivity = 26.4805 dB, peak side lobe level =-20.4 dB, and complexity = 100%, while for the proposed array with $R = 7.025$, these values were 2.7587, 25.0438 dB, -21.4 dB, and 66.22%, respectively. These mean that the proposed array was able to provide better taper efficiency, comparable directivity, average side lobes, and a great reduction in the array complexity.

In the future work, the thinning process may be included and combined with the optimization process of the proposed array to further reduce the relatively large number of the adaptive elements outside the circular boundary. Its effectiveness in the wireless monitoring applications will also be investigated [25].

REFERENCES

1. Kahrilas, P. J., "HAPDAR — An operational phased array radar," *Proc. IEEE*, Vol. 56, No. 11, 1967–1975, 1968.
2. Brookner, E., *Aspects of Modern Radar*, 1st Edition, Artech House, Norwood, MA, 1988.
3. "Raytheon datasheet," Sea-Based X-Band Radar (SBX) for Missile Defence, Raytheon Datasheet [Online], available: www.raytheon.com/capabilities/rtnwcm/groups/rms/documents/content/rtn_rms_ps_sbx_datasheet.pdf, accessed 3 June 2020.
4. Eiscat3d science report [Online], available: http://www.eiscat3d.se/sites/default/files/ EISCAT3D_ScienceCase_v2.pdf, accessed 3 June 2020.
5. Mailloux, R. J. and E. Cohen, "Statistically thinned arrays with quantized element weights," *IEEE Trans. Antennas Propag.*, Vol. 39, No. 4, 436–447, Apr. 1991.
6. Keizer, W. P. M. N., "Large planar array thinning using iterative FFT techniques," *IEEE Trans. Antennas Propag.*, Vol. 57, No. 10, 3359–3362, Oct. 2009.
7. Haupt, R. L., "Thinned arrays using genetic algorithms," *IEEE Trans. Antennas Propag.*, Vol. 42, No. 7, 993–999, Jul. 1994.

8. Sallam, T. and A. M. Attiya, "Low sidelobe cosecant-squared pattern synthesis for large planar array using genetic algorithm," *Progress In Electromagnetics Research M*, Vol. 93, 23–34, 2020.
9. Kodgirwar, V. P., S. Deosarkar, and K. Joshi, "Design of adaptive array with E-shape slot radiator for smart antenna system," *Progress In Electromagnetics Research M*, Vol. 90, 137–146, 2020.
10. Mohammed, J. R., "Thinning a subset of selected elements for null steering using binary genetic algorithm," *Progress In Electromagnetics Research M*, Vol. 67, 147–157, 2018.
11. Robinson, J. and Y. Rahmat-Samii, "Particle swarm optimization in electromagnetics," *IEEE Trans. Antennas Propag.*, Vol. 52, No. 2, 397–407, Feb. 2004.
12. Recioui, A., "Sidelobe level reduction in linear array pattern synthesis using particle swarm optimization," *Journal of Optimization Theory and Applications*, Vol. 153, No. 2, 497–512, 2012.
13. Ojaroudi Parchin, N., H. J. Basherlou, Y. I. A. Al-Yasir, and R. A. Abd-Alhameed, "A design of antenna array with improved performance for future smart phones," *Progress In Electromagnetics Research C*, Vol. 101, 1–12, 2020.
14. Recioui, A., "Concentric ring arrays optimization using the spiral inspired technique," *Algerian Journal of Signals and Systems*, Vol. 3, No. 1, 10–21, Mar. 2018.
15. Zhengdong, Q., B. Yechao, W. Qiong, Z. Xinggan, and C. Hao, "Optimal synthesis of reconfigurable sparse arrays via multi-convex programming," *IET Radar, Sonar & Navigation*, 2020, DOI: 10.1049/iet-rsn.2019.0236.
16. Lopez, P., J. A. Rodriguez, F. Ares, and E. Moreno, "Low-sidelobe patterns from linear and planar arrays with uniform excitations except for phases of a small number of elements," *Electronics Letters*, Vol. 37, No. 25, 1495–1497, Dec. 2001.
17. Mohammed, J. R., "Design of printed Yagi antenna with additional driven element for WLAN applications," *Progress In Electromagnetics Research C*, Vol. 37, 67–81, 2013.
18. Compton, R. T., *Adaptive Antennas*, Prentice Hall, New Jersey, 1988.
19. Li, Y., L. M. Vicente, K. C. Ho, and Y. H. Leung, "A study of the partially adaptive concentric ring array," *Circuits Systems and Signal Processing*, Vol. 27, No. 5, 733–748, Oct. 2008.
20. Sayidmarie, K. H. and J. R. Mohammed, "Performance of a wide angle and wideband nulling method for phased arrays," *Progress In Electromagnetics Research M*, Vol. 33, 239–249, Oct. 2013.
21. Mohammed, J. R., "Optimal null steering method in uniformly excited equally spaced linear array by optimizing two edge elements," *Electronics Letters*, Vol. 53, No. 11, May 2017.
22. Mohammed, J. R. and K. H. Sayidmarie, "Sidelobe cancellation for uniformly excited planar array antennas by controlling the side elements," *IEEE Antennas and Wireless Propagation Letters*, Vol. 13, 987–990, 2014.
23. Mohammed, J. R. and K. H. Sayidmarie, "Performance evaluation of the adaptive sidelobe canceller with various auxiliary configurations," *AEÜ International Journal of Electronics and Communications*, Vol. 80, 179–185, 2017.
24. Mohammed, J. R., "Element selection for optimized multi-wide nulls in almost uniformly excited arrays," *IEEE Antennas and Wireless Propagation Letters*, Vol. 17, No. 4, 629—632, Apr. 2018.
25. Castorina, G., L. Di Donato, A. F. Morabito, T. Isernia, and G. Sorbello, "Analysis and design of a concrete embedded antenna for wireless monitoring applications," *IEEE Antennas and Propagation Magazine*, Vol. 58, No. 6, 76–93, 2016.